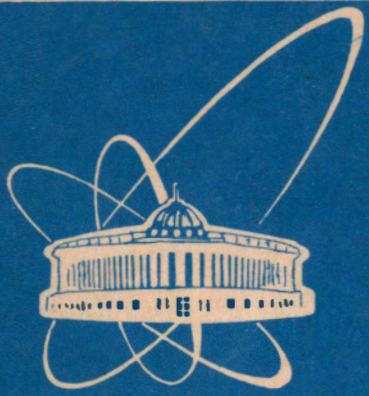

ОБЪЕДИНЕННЫЙ
ИНСТИТУТ
ЯДЕРНЫХ
ИССЛЕДОВАНИЙ

Дубна

E17-95-324

S.Frauendorf[1], V.V.Pashkevich

THERMODYNAMICS AND DECAY OF LIQUID ALKALI CLUSTERS

Contribution to: NATO Advanced Study Institute,
International School of Solid State Physics,
6th Course: Large Clusters of Atoms and Molecules,
E.Majorana Centre for Scientific Culture,
Erice/Sicily: June 19—29, 1995

[1]Institute for Nuclear and Hadronic Physics, Research Center Rossendorf Inc.,
PB 510119, D-01314 Dresden, Germany

1995

Фрауендорф С., Пашкевич В.В.
Е17-95-324

Термодинамика и распад жидких щелочных кластеров

Сформулирован метод оболочечных поправок для расчета формы и свободной энергии нагретых жидких щелочных кластеров. Минимизируя свободную энергию одновременно по пяти параметрам деформации, рассчитали равновесные формы кластеров натрия с массой от 100 до 700. Найдено, что в середине открытых оболочек сильные отклонения от сфероидальной формы, включая зеркально-асимметричные формы, не исчезают даже при $T = 700$ K. Предложено соотношение, связывающее скорость испарения атомов со свободной энергией. Скорость испарения сравнивается с соответствующей величиной, полученной в рамках ансамбля гармонических осцилляторов.

Работа выполнена в Лаборатории теоретической физики им.Н.Н.Боголюбова ОИЯИ и Институте ядерной и адронной физики (Исследовательский центр в Россендорфе).

Препринт Объединенного института ядерных исследований. Дубна, 1995

Frauendorf S., Pashkevich V.V.
E17-95-324

Thermodynamics and Decay of Liquid Alkali Clusters

The shell correction method is formulated to calculate the shapes and free energies of hot liquid alkali clusters. The equilibrium shapes of Na clusters with mass 100 to 700 are calculated by minimizing the free energy with respect to up to five deformation parameters simultaneously. For $T = 700$ K strong deviations from spheroidal shape including reflection asymmetric shapes are found to survive in the center of the open shells. An expression is suggested that relates the rate for evaporation of atoms to the free energy. It is compared with the rate constant based on the ensemble of harmonic oscillators.

The investigation has been performed at the Bogoliubov Laboratory of Theoretical Physics, JINR and at the Institute for Nuclear and Hadronic Physics (Research Center Rossendorf Inc.).

Preprint of the Joint Institute for Nuclear Research. Dubna, 1995

1. Introduction

The ionic degrees of freedom dominate the thermodynamical properties of liquid clusters. As the statistical description of thermodynamics in terms of these degrees of freedom is already a rather complex problem for classical bulk liquids, such a description of large liquid clusters is expected to be even more difficult. Thus, a more phenomenological approach appears to be useful. As a suitable phenomenological model we suggest to consider a small, but macroscopic droplet of liquid alkali metal, whose thermodynamical properties are taken from experiment. On the other hand, the shell structure appearing in the system of the delocalized valence electrons influences many properties of alkali clusters in a significant way [1]. Obviously these shell effects can be described only in terms of the microscopic degrees of freedom of the valence electrons. The shell correction method (SCM) developed in nuclear physics [2] presents a possibility to merge these two apparently conflicting aspects into a unified description of liquid alkali clusters. In section 2 we develop the SCM for alkali clusters at finite temperature, in section 3 calculations of the free energies and shapes of sodium clusters for different temperatures are presented and in section 4 we discuss some consequences for the evaporation of neutral atoms.

2. Shell correction for finite temperature

The SCM for alkali clusters at finite temperatures has been suggested by us in ref. [3]. It is formulated for the free energy $F(T,N)$ of a cluster with mass number N at a temperature T. Since F is a thermodynamical potential all other thermodynamic quantities may be calculated by taking the derivatives appropriate for the process considered. The total free energy is written as the sum

$$F = F_{LD} + \delta F \tag{1}$$

where F_{LD} is the free energy of a classical drop of liquid alkali metal, consisting of N atoms, and δF is the shell correction, which accounts for the shell structure in the valence electron system.

Let us first consider the droplet free energy. Restricting to the case of neutral clusters,

$$F_{LD} = fN + 4\pi r_S^2 N^{2/3} \sigma S(\alpha, \alpha_\mu). \tag{2}$$

The first, "volume" term is determined by the specific free energy f. The second, "surface" term is the product of the surface tension σ and the surface area. The function $S(\alpha, \alpha_\mu)$ is the area of the surface enclosing the unit volume. It depends on the deformation parameters $\alpha, \alpha_3, \alpha_4, ...$, which fix the quadrupole, octupole, hexadecapole and higher deformations, respectively [1]. The Wigner - Seitz radius r_s, the specific free energy f^* and the surface tension σ are assumed to be given by the experimental values at standard pressure $p_o = 1\ atm$, as quoted in the tables (e. g. in [4, 5]). [2]

The central assumption of the our model is that the scaling of F_{LD} with the number of atoms N holds down to a few tens of atoms. It is noted that the surface term, which is usually called "surface energy", is actually a free energy, since the experiments to measure it are always carried out at a fixed temperature.

The temperature dependence of the droplet is parametrized as follows. Usually, the tables quote the specific heat c_p as a polynomial in T. One may safely ignore the difference between c_p and c_V for the liquid, since the volume work

[1] This is only correct for not too large deformation. The accurate definition of the deformation parameters can be found in ref. [6].

[2] In using these parameters for clusters in the vacuum, we assume that the presence of the vapor changes them only insignificantly. This is an uncritical assumption, since the vapor density of most materials is very low at standard pressure (the critical point is far away).

$p_o v$ is negligible compared to c. Using a third order polynominal, as in [5], the specific heat of the liquid reads

$$c(T) = c_0 + c_1 T + c_2 T^2. \tag{3}$$

By integration one obtains the specific energy

$$e(T) = e_0 + c_0 T + \frac{1}{2} c_1 T^2 + \frac{1}{3} c_2 T^3. \tag{4}$$

Integrating c/T gives the specific entropy

$$s(T) = s_0 + c_0 \ln T + c_1 T + \frac{1}{2} c_2 T^2, \tag{5}$$

and the specific free energy is given by

$$f(T) = e(T) - Ts(T). \tag{6}$$

The surface tension can be approximated by

$$\sigma(T) = \sigma_0 - \sigma_1 T, \tag{7}$$

and the Wigner - Seitz radius by

$$r_s(T) = \left[\frac{3v(T)}{4\pi}\right]^{1/3} = r_0 + r_1 T + r_2 T^2. \tag{8}$$

Here, $v(T)$ is the specific volume. For liquid sodium the parameters are [4, 5]: $c_0 = 4.405, c_1 = -26.7eV^{-1}, c_2 = 172.3eV^{-2}, \sigma_0 = 0.0147eV\mathring{A}^{-2}, \sigma_1 = 0.072\mathring{A}^{-2}, r_0 = 2.065\mathring{A}, r_1 = 1.322\mathring{A}eV^{-1}, r_2 = 9.11\mathring{A}eV^{-2}, e_0 = -1.13eV$ and $s_0 = 23.721$.

The shell correction δF is defined as the difference

$$\delta F = F_e - \tilde{F}_e. \tag{9}$$

Here, F_e is the free energy of N electrons in the average potential U, which is generated by them and by the ions, and $\tilde{F}_e$ is the free energy of N electrons distributed over a modified spectrum of U, which does not have the level bunching. This "smooth" spectrum, from which the shell structure is eliminated, will be defined below. The energies e_i of the valence electrons are the eigenvalues of the single particle hamiltonian h, containing the Woods Saxon potential

$$h = \frac{\vec{p}^2}{2m} + U_o[1 + exp(l(\vec{x})/d)]^{-1}. \tag{10}$$

Here, m is taken to be the free electron mass and $l(\vec{x})$ measures the distance of a point $\vec{x}$ from the equipotential surface $U(\vec{x}) = 1/2U_o$. The shape of this surface is taken to be the same as the one used to calculate the surface area $S(\alpha, \alpha_\mu)$ in the liquid drop part. The volume enclosed by the equipotential surface is kept constant to

$$V_p = \frac{4\pi}{3} R_P^3, \quad R_P = r_s N^{1/3} + \delta. \tag{11}$$

The radius of the potential exceeds the cluster radius by δ in order to account for the electronic spill-out. For sodium the diffuseness of the surface is chosen to be $d = 0.74\mathring{A}$, the spill-out $\delta = 0.63\mathring{A}$ and the depth of the well U_o=-6eV. The parameters are obtained from a fit to $T = 0$ spherical jellium Kohn - Sham calculations (for details cf. ref. [6]).

The calculation of the free energy is based on the *canonical* ensemble of the valence electrons. This is important, since typical experiments study mass selected cluster beams. The free energy of N independent electrons is calculated as

$$F_e = \lambda N - T \ln[\frac{1}{L} \sum_{l=1}^{L} e^{i\frac{2\pi lN}{L}} \prod_j [1 + e^{-\frac{e_j - \lambda}{T} - i\frac{2\pi l}{L}}]] \tag{12}$$

For $L \to \infty$ this is an exact expression. [3] We find that $L = 16$ gives the canonical free energy with an relative accuracy better than 10^{-3}, provided λ is chosen such that the mean value of the particle number in the corresponding grand canonical ensemble is equal to N. Our method to evaluate the canonical partition function is different from the one suggested by Brack et al. [9]. It seems to be numerically faster. The accuracy can be controlled by changing L.

The smooth free energy $\tilde{F}_e$ is calculated from a set of non bunched levels $\tilde{e}_i$, by means of eq. (12). This smooth spectrum is constructed from the smooth density of single particle states, $2\tilde{g}(e)$, which is calculated by means of the Strutinsky averaging procedure from the spectrum e_i (for the detailed definition of $\tilde{g}(e)$, cf. ref. [2]). Solving numerically the equations

$$i = \int_{-\infty}^{\lambda_i} 2\tilde{g}(e)de \tag{13}$$

the set of chemical potentials $\lambda_i, i = 1, 2...$ is found. The smooth spectrum is generated by the integrals

$$\tilde{e}_i = \int_{\lambda_{i-1}}^{\lambda_i} 2\tilde{g}(e)ede, \tag{14}$$

[3] This can be seen best by using the projected statistics representation of refs. [7, 8].

where $\lambda_{-1} = -\infty$. The spectrum is constructed such that it fulfills the relation

$$\sum_{i=1}^{N} \tilde{e}_i = \tilde{E} = \int_{-\infty}^{\lambda_N} 2\tilde{g}(e)ede, \tag{15}$$

where $\tilde{E}$ is the smooth energy introduced by Strutinsky [2].

3. Shapes and free energies of sodium clusters

We have minimized the free energy simultaneously with respect to $\alpha, \alpha_\mu, \mu = 3, 4, 5, 6$ for all even Na clusters in the mass range $90 \leq N \leq 310$ and for the pairs α, α_4 and α, α_3 in the mass range $310 \leq N \leq 730$. Three different temperatures, $T = 0, 0.04$ and 0.06 eV, i.e $0°, 465°$ and $697° K$ have been studied. The equilibrium deformations are presented in figures 1, 2 and 3.

We also display in figures 1 and 3 the shell contribution to the free energy F_{SH}, which is defined as as the free energy at the minimum relative to the free energy of the spherical drop:

$$F_{SH} = F - F_{LD}(\alpha = 0, \alpha_\mu = 0) \tag{16}$$

Note, in fig. 3 the zero line of F_{LD} is not horizontal!

The deformation drastically lowers the free energies in the open shells. Though the largest contribution (1 - 2 eV for $T = 0$) comes from the quadrupole deformation, the higher multipoles also contribute significantly. For $T = 0$ the octupole contributes up to $0.5eV$ and the hexadecapole up to $0.3\ eV$. For selected clusters we minimized the free energy with respect to the multipoles up to $\mu = 10$. The energy gain due to $\mu = 7, 8, 9, 10$ is typically less than a few 10 meV. Within our five dimensional family $\mu \leq 6$ the axial shapes can be considered as relaxed.

As cluster deformation is a consequence of the shell structure, it is suppressed by the thermal fluctuations. Figs. 1, 2 and 3 demonstrate that this does not occur as a gradual decrease of the magnitude of the deformation. Rather, the regions of spherical shape around the magic numbers are expanding with T and N. It is also seen that the role of the higher multipoles ($\alpha_\mu, \mu \geq 3$) remains as important as for zero temperature. In other words, the average shapes for $T \neq 0$ are about the same as for $T = 0$, provided the clusters are not spherical. One may say that "parts of the deformed regions melt away". Even for $N \approx 600$ and $T = 700° K$ substantial islands of deformation are left in the center of open shells.

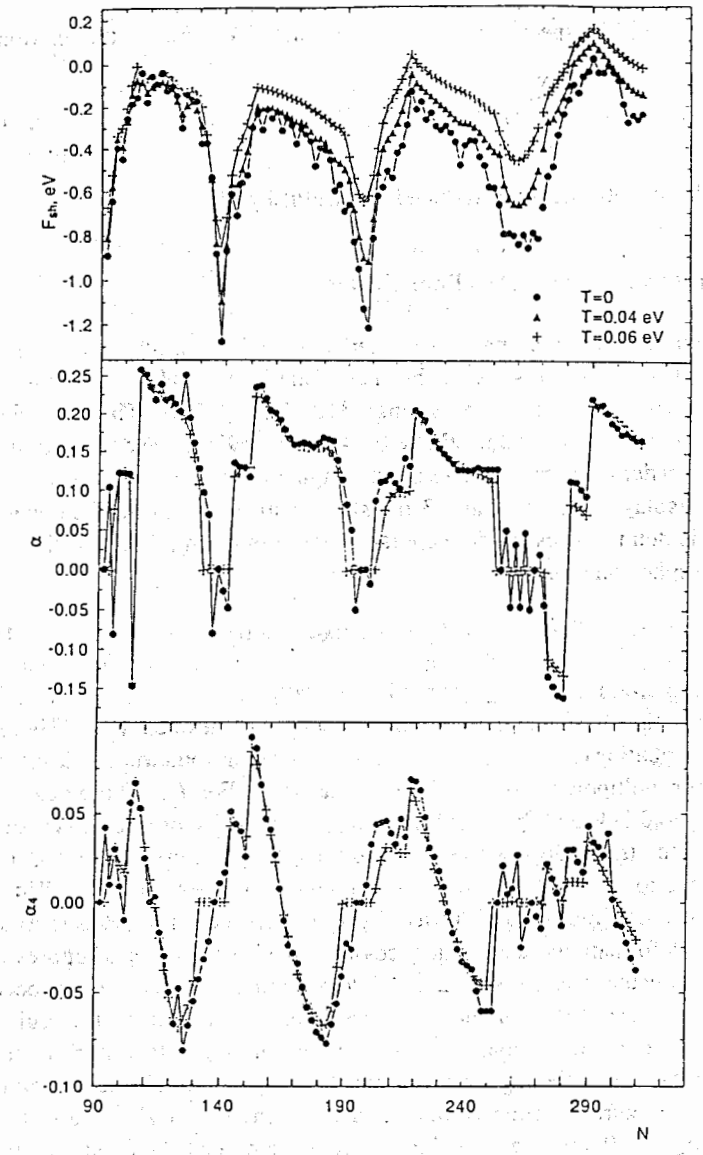

Figure 1. Shell contribution F_{SH} to the free energy after minimization with respect to five deformation parameters and the equilibrium deformation parameters α and α_4 of liquid Na clusters in the mass range $90 \leq N \leq 310$.

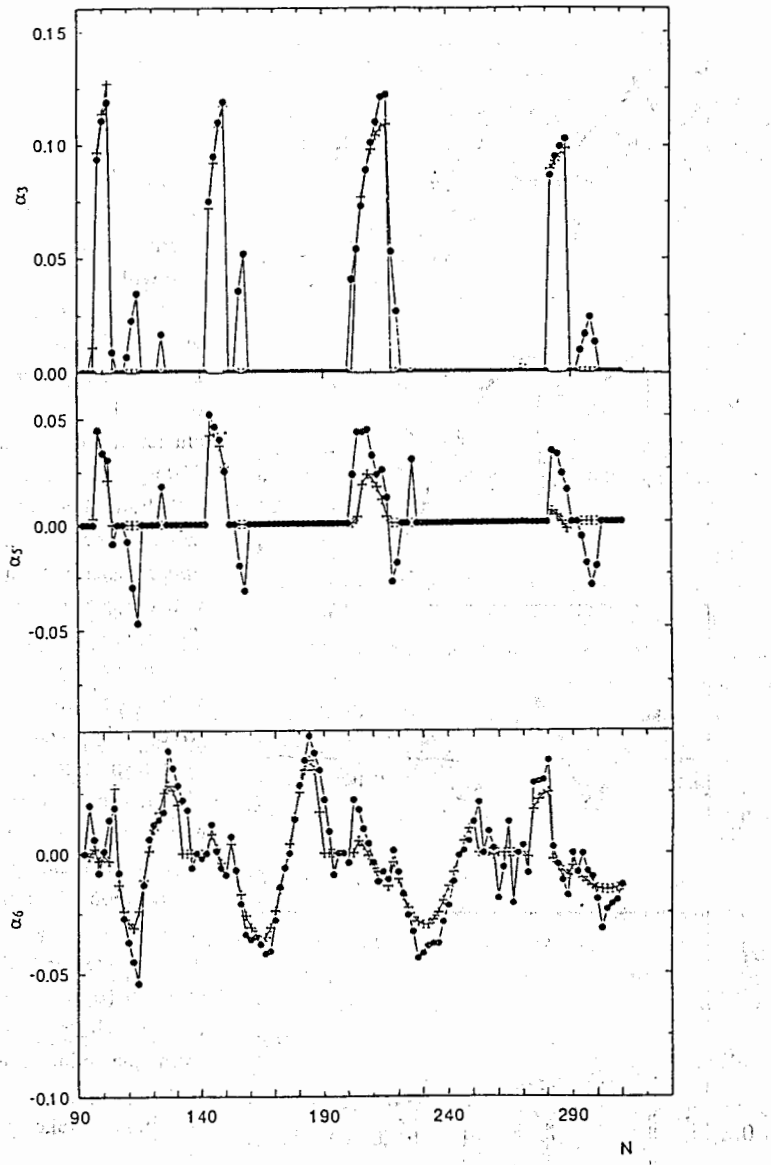

Figure 2. As figure 1 for the equilibrium deformation parameters α_3 , α_5 and α_6.

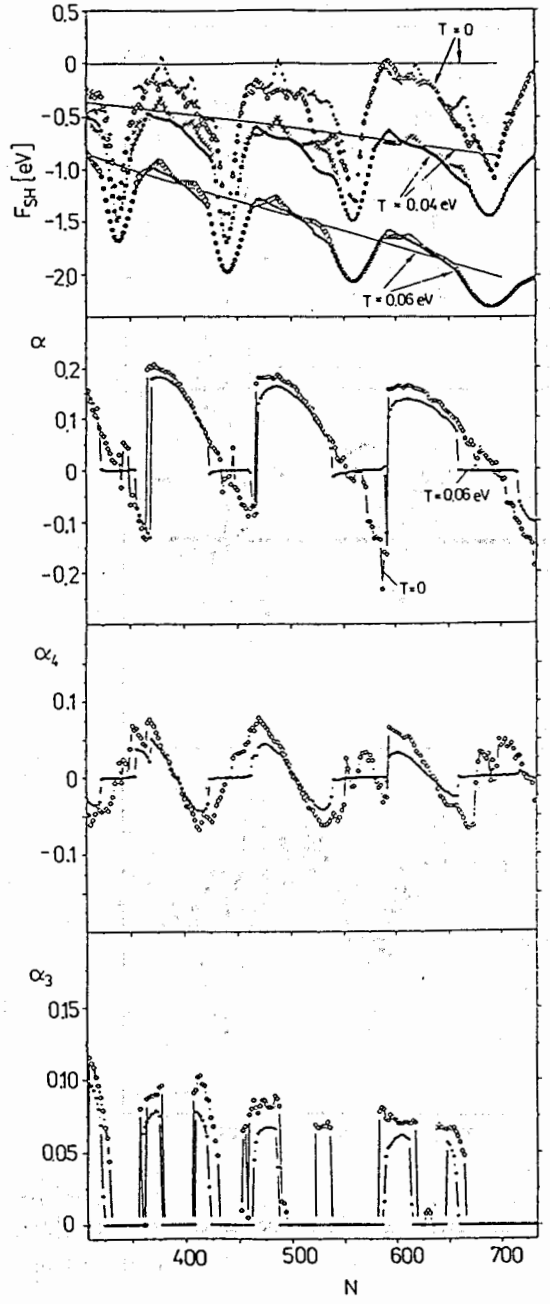

Figure 3. Shell contribution F_{SH} to the free energy after minimization with respect to pairs of deformation parameters and the equilibrium deformation parameters α, α_3 and α_4 of liquid Na clusters in the mass range $310 \leq N \leq 730$. The full drawn lines are the zero lines for F_{SH}. In the upper panel the curves with the spike in the middle of each shell are results of the minimization with respect to the pair (α, α_3) the other ones with respect to (α, α_4). The deformation parameters are shown only for $T = 0$ (diamonds) and $T = 0.06$ eV (stars). Only the α - values from the minimization with respect to (α, α_4) are included. The α - values from the minimization with respect to (α, α_3) are similar. Taken from ref. [3].

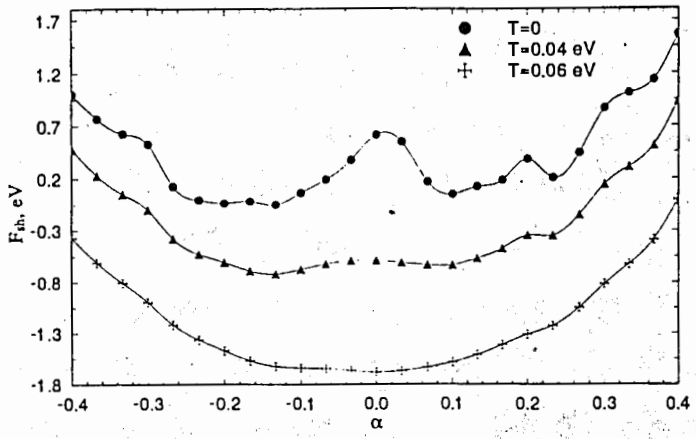

Figure 4. The free energy of Na_{586} as a function of the deformation parameter α. The quantity F_{SH} is defined in the same way as in figure 3.

Such a behavior is a consequence of the fact that the surface $\delta F(\alpha, \alpha_\mu T)$ is similar to the surface $\delta E(\alpha, \alpha_\mu)$ at $T = 0$. Only the scale of the relief is reduced and it is smoothed. The deformed minima of the clusters near the magic N are relatively shallow. At finite T they become so shallow that they can no longer compete with the term F_{LD}, which drives towards spherical shape (cf. fig. 4). On the other hand, in the center of the open shells the minima of δF are sufficiently deep such that the reduction of their depth is not enough to make F_{LD} competitive. They will remain in the total F surfaces, shifted only to slightly reduced deformation (cf. fig. 5).

The thermal fluctuations tend to wash out the shell structure [9]. The difference between the calculations at $T = 0$ and $T = 700°K$ increases with the mass number N. This is expected, because the parameter controlling the suppression of the shell structure is the ratio $T/\hbar\omega$, where $\hbar\omega \sim 4N^{-1/3}eV$ is the spacing of the shells. Thus, a temperature of $700°K$ is rather low for $N \approx 100$ and the amplitude of the shell modulations is about the same as for $T = 0$. For $N > 300$ the same temperature causes a significant suppression of the shell structure.

The deformations shown in figures 1, 2 and 3 represent the *average* shape of the ensemble. There are thermal fluctuations around them. The amplitude of these fluctuation is

$$\Delta\alpha \sim \sqrt{T(d^2F/d\alpha^2)^{-1}} \qquad (17)$$

In the centers of the spherical and of the deformed regions the shell correction δF

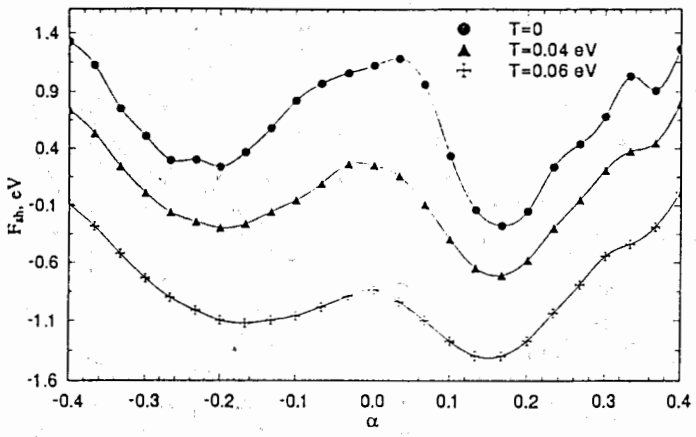

Figure 5. The free energy of Na_{500} as a function of the deformation parameter α. The quantity F_{SH} is defined in the same way as in figure 3.

increases the curvature and, as a consequences, reduces the thermal fluctuations (compare fig. 4 and 5). In the transitional regions, where the deformation melts, the contribution of $d^2\delta F/d\alpha^2$ to the total value of $d^2F/d\alpha^2$ is small. There, the thermal fluctuations are much larger, of the order of the fluctuations of the classical drop.

Fig. 6 illustrates the importance of the higher multipoles by displaying the actual cluster shapes at zero temperature. The shapes for higher temperature are almost the same, except that the regions of spherical clusters around the magic numbers expand. It is seen that the shapes of most clusters are rather different from spheroids, which appear only for a restricted number of clusters in the center of the deformed region. Instead, the sequence of spherical - pear like - lemon like - spheroidal - barrel like - spherical shapes is repeated in each shell.

In order to check the predictions of the SCM it would be interesting to measure the ionization potentials for the alkali cluster with a mass larger than 100. Their local variations may serve as an indication of the predicted melting away of the shell structure.

The measurement of the plasmon resonance for heavy mass selected clusters should provide evidence for the predicted survival of deformation. So far there exists only a measurement of the plasmon resonance in K clusters with masses distributed around 500 and temperatures between $600°K$ and $800°K$ [10]. No splitting of the resonance has been observed. This could be taken as an evidence that the average quadrupole deformation should be small. The SCM predicts

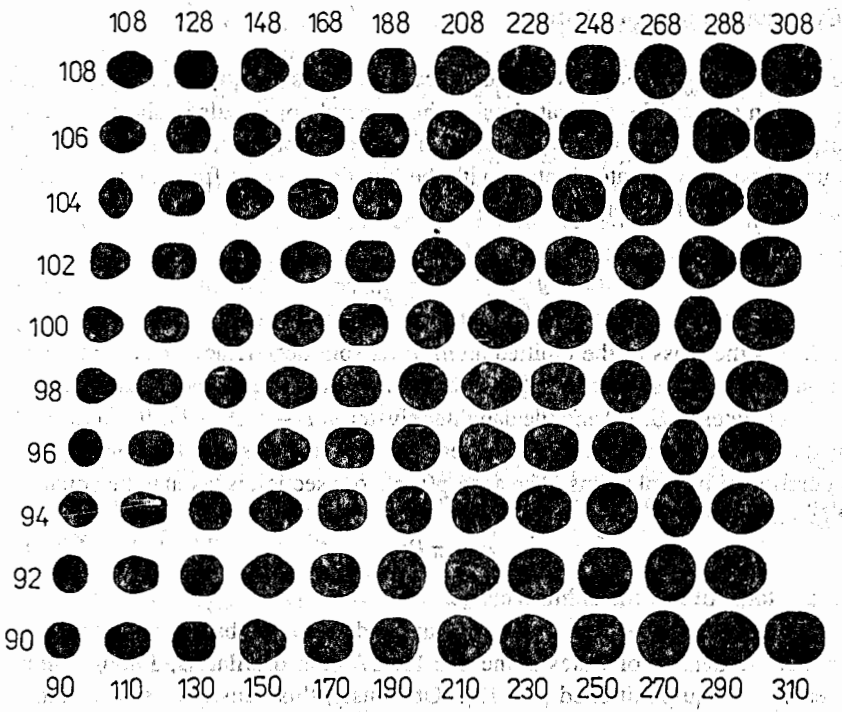

Figure 6. Shapes of the even Na clusters in the mass range $90 \leq N \leq 310$. The clusters are ordered according to their electron number N from the left to the right. The values of N are given for the clusters on the outer border of the figure. The symmetry axes lie horizontally.

substantial quadrupole deformations around $N = 500$ (cf. fig. 3). According to fig. 5, the shape fluctuations at a temperature of 0.06 eV should not be large enough to destroy the average quadrupole deformation and a splitting of the resonance should be seen. As will be discussed below, the evaporation spectra seem to contain evidence for deformation around mass 500, in accordance with the calculations. The reason of this discrepancy is not clear at this point. The poor mass resolution or differences between Na and K may play a role.

In the following we will discuss how the results of the SCM can be used to calculate decay rates of liquid clusters.

4. Evaporation of neutral atoms

The evaporation of neutral atoms can be considered as a statistical process. The evaporation rate can be estimated using the principle of detailed balance, which Weiskopf [11] applied for the evaporation of neutrons from nuclei. The probability per unit time to evaporate an atom with the kinetic energy ε from a cluster with mass number N and energy E is [11]

$$W d\varepsilon = g\frac{m\sigma}{\pi^2\hbar^3}\varepsilon\frac{\rho(E-\varepsilon, N-1)}{\rho(E,N)}d\varepsilon. \tag{18}$$

Here, m is the mass of the emitted atom, g its spin degeneracy and σ the cross section for the inverse reaction of absorbing one atom. The mother cluster has the density of states $\rho(E,N)$ and the daughter cluster $\rho(E-\varepsilon, N-1)$. It is assumed that there is no barrier for the atom leaving the cluster, since we consider the evaporation of neutral atoms. The absorption cross section is taken to be equal to the geometric one

$$\sigma = \pi R^2, \tag{19}$$

i. e. an atom sticks when it hits a cluster.

Rate constants have been derived and applied to clusters based on the assumption that the density of states is the one for $3N-6$ oscillators, among which the energy is equipartitioned [12, 13]. Obviously, this density of states cannot be very accurate for liquid clusters. The ions move through the cluster instead of oscillating around fixed positions in a molecular skeleton. We do not use an explicit model for the ions, rather we exploit a relation between the entropy and the density of states that has been derived in refs. [14, 15] and represents an approximation to the microcanonical ensemble

$$\rho(E,N) = \frac{1}{T(E,N)\sqrt{2\pi C(E,N)}}e^{S(E,N)}. \tag{20}$$

The entropy $S(T,N)$, the energy $E(T,N)$ and the heat capacity $C(T,N)$ are obtained from the free energy $F(T,N)$ by the standard thermodynamical relations for a *free* cluster, only in contact with a heat bath.

$$S(T,N) = -\frac{\partial}{\partial T}F(T,N) \tag{21}$$

$$E(T,N) = F(T,N) + TS(T,N) \tag{22}$$

$$C(T,N) = \frac{\partial}{\partial T}E(T,N) = T\frac{\partial}{\partial T}S(T,N). \tag{23}$$

Inverting eq. (22) determines the temperature $T(E,N)$ as a function of the energy and provides $C(E,N)$ and $S(E,N)$. The preceding relations permit to calculate the density of states from the SCM free energy $F(T,N)$, which has been introduced in section 2. It should be underlined that *the droplet expression for F_{LD} represents a phenomenological model for the density of states of both the ions and the valence electrons.* Since its parameters are adjusted to the experimental thermodynamic properties it is expected to be more realistic than the model of $3N-6$ oscillators. The shell correction δF determines the modulation of the density of states by the shell structure.

Combining eqs.(18) and (20) the evaporation rate becomes [15]

$$k = g\frac{mR^2}{\pi\hbar^3}T(E,N)T(E,N-1)\sqrt{\frac{C(E,N)}{C(E,N-1)}}e^{S(E,N-1)-S(E,N)} \tag{24}$$

A similar expression without a shell correction has been derived in ref. [16]. For large clusters one may assume that the temperature does not change very much when one atom is emitted. Then

$$S(E,N-1) - S(E,N) \approx -\frac{F(T,N-1)-F(T,N)}{T} \equiv \frac{\Delta_1 F(T,N)}{T} \tag{25}$$

and the rate takes the simple form [15, 17]

$$k = g\frac{mR^2}{\pi\hbar^3}T^2 e^{-\Delta_1 F(T,N)/T}. \tag{26}$$

Tab. 1 quotes evaporation rates for sodium that are calculated neglecting the shell correction, i. e. $F = F_{LD}$. It is seen that for $N > 100$ the assumption of a small change of temperature after the emission of one atom and, as a consequence, expression (26) become quite accurate. Below mass 100 one cannot neglect the change of the temperature and should use the expression (24).

Analyzing experimental evaporation spectra it is a popular approach to use the density of states of the system of $3N-6$ harmonic oscillators $\rho_E(E^*, N)$, which depends only on the thermal energy,

$$E^* = E - E_o(N), \tag{27}$$

where $E_o(N)$ is the ground state energy. All effects of the shell structure are assumed to be represented by the variation of $E_o(N)$, since ρ_E is a smooth function of N. This approach results in Engelking's evaporation rate [12]

$$k_E = g\frac{mR^2}{\pi\hbar^3}(\hbar\omega)^3\frac{(E^*-D(N))^{3N-8}}{(E^*)^{3N-7}}, \tag{28}$$

TABLE 1. Comparison of different evaporation rates. The decimal logarithm of the rates is quoted, where the rates are in units s^{-1}. The energies are given in eV and the temperatures in meV. The column k_D presents the droplet rate (24) calculated assuming $T = 50\ meV$ for the mother. The thermal energies of the mother and daughter, as obtained from the droplet model, are given in the column E^*. The column k_G quotes the rate expression (26), evaluated for $T = 50\ meV$. The column k_E presents Engelking's rate (28), where for each pair of N the upper line is calculated for the thermal energy as given in the column E^* and the lower line is calculated for $T = 50\ meV$. The column T_E quotes the temperatures in Engelking's model, corresponding the case when E^* is chosen to be equal to the droplet value for the mother. The frequency the oscillators in eq. (28) is equal to the Debeye value $\hbar\omega = 12.8\ meV$. In all calculations only the liquid drop free energy has been used and $g = 1$.

N	E^*	$\log k_D$	$\log k_G$	T	$\log k_E$	T_E
20	4.04	5.64	6.50	50	9.40	75
19	3.09			40	5.89	61
50	9.99	6.05	6.41	50	9.25	69
49	9.00			46	6.71	64
100	19.85	6.21	6.40	50	9.23	68
99	18.84			48	6.93	65
500	98.35	6.50	6.54	50	9.33	66
499	97.28			50	7.20	65
10^3	196.15	6.62	6.64	50	9.43	66
	195.07			50	7.32	65
10^4	1950.30	7.10	7.12	50	9.88	65
	1949.19			50	7.78	65

where the ground state separation energies

$$D(N) = E_o(N-1) - E_o(N) \tag{29}$$

have been introduced. There are two inherent assumptions that we would like to discuss: The oscillator model for the density of states and the absence of shell structure in E^*.

Let us start from the first. Table 1 compares the our droplet rate, which is obtained by setting $F = F_{LD}(sphere)$, with Engelking's expression, in which the separation energies $D(N)$ have been set equal to the spherical droplet values at $T = 0$. The difference between the two rates consists only in the treatment of the thermal excitation. The values of k_E in the upper line of the fifth column of table 1 are obtained assuming that the mother cluster has the same internal

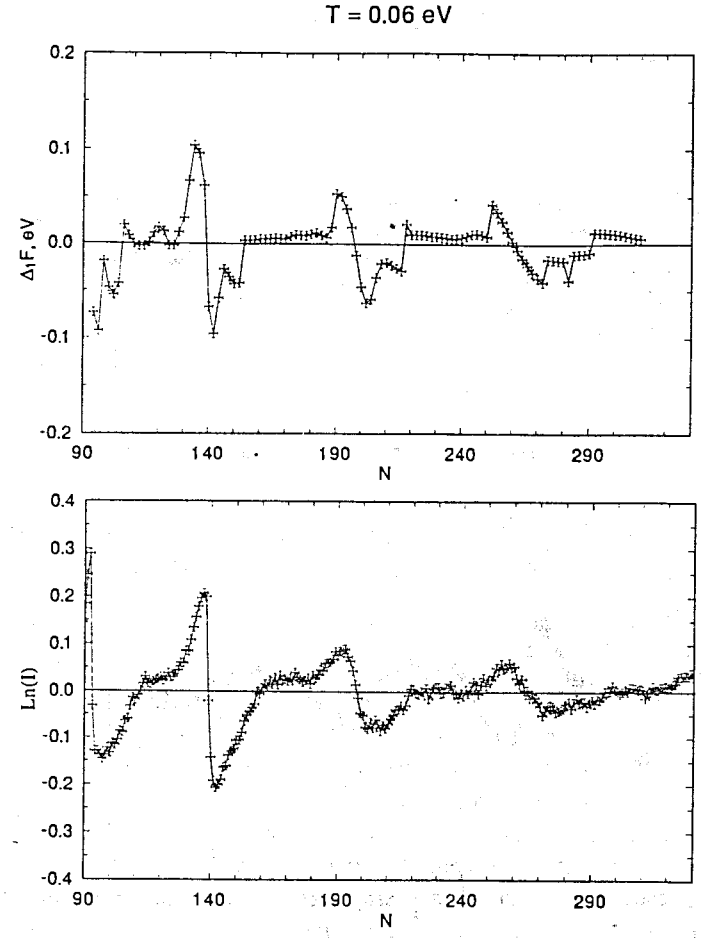

Figure 7. Differences of the free energies (upper panel) and logarithm of the relative experimental intensities (lower panel) as determined in ref. [20, 21] for Na clusters in the mass range $90 \leq N \leq 310$. The quantity $\Delta_1 F(N) = (F_{SH}(T, N-2) - F_{SH}(T, N))/2$ is displayed for $T = 0.06\ eV$.

energy E^* as the droplet (quoted in the second column of table 1). The droplet rate is three to four orders of magnitude smaller than Engelking's estimate. The origin of the difference is the smaller heat capacity of the system of oscillators. At $T = 50\ meV$, the specific heat of sodium is $c = 3.5$ to be compared with 3 for the system of harmonic oscillators. As a consequence the temperature is higher

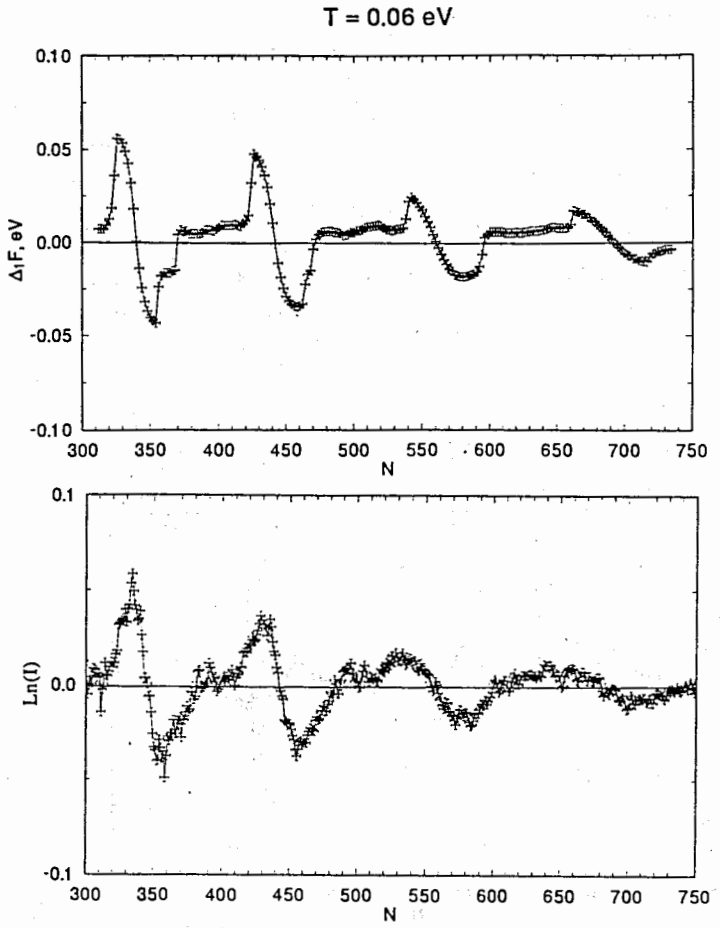

Figure 8. Differences of the free energies (upper panel) and logarithm of the relative experimental intensities (lower panel) as determined in ref. [20, 21] for Na clusters in the mass range $310 \leq N \leq 730$. The quantity $\Delta_1 F(N) = (F_{SH}(T, N-2) - F_{SH}(T, N))/2$ is displayed for $T = 0.06\, eV$

in the latter. Since more atoms are excited to energies large enough to separate from the cluster, the evaporation rate is strongly enhanced. The larger specific heat of the liquid is a consequence of the strong anharmonicities in the vibrational amplitudes that occur when the material melts. If in an experiment the thermal energy E^* would be known, one could directly calculate the separation energies

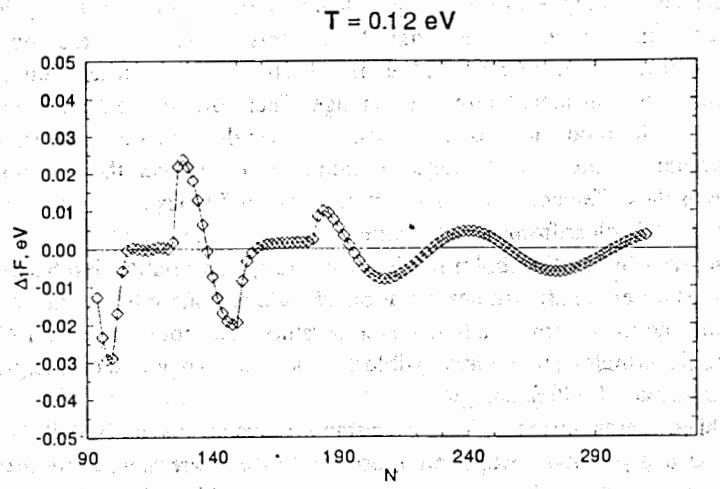

Figure 9. Differences of the free energies for Na clusters in the mass range $310 \leq N \leq 730$. The quantity $\Delta_1 F(N) = (F_{SH}(T, N-2) - F_{SH}(T, N))/2$ is displayed for $T = 0.12\, eV$

$D(N)$ from the measured evaporation rates. The different heat capacities of the system of harmonic oscillators and the droplet would lead to different values of $D(N)$. If one chooses $D(N)$ such that Engelking's rate becomes equal to the droplet value given in the table 1, one finds $D(500) = 1.49\, eV$ instead of the value $1.06\, eV$. The latter value corresponds to the zero temperature liquid drop energies E_o and is used in the calculation of the droplet rate. An experiment, in which a single photon of definite energy is absorbed, would permit to distinguish between these two models. As seen in table 1, our droplet rate and Engelking's rate are not very different when taken at the same temperature. Qualitatively this is explained by the fact that the thermal activation is the same in both cases. The smaller value of E^* for the oscillator model does not come into play. Thus, in experiments that fix the temperature, like the analysis of the ratios of monomer and dimer yields carried out in refs [18, 19], the droplet rate and Engelking's rate agree much better. As discussed in detail in ref. [15], the separation energies $D(N)$ derived from the ratios of the evaporation yields agree within $100\, meV$. For example, assuming equal ratios between the dimer and monomer intensities for N=500 the separation energies derived from the two models would differ by $80\, meV$.

The second assumption, that the electronic shell structure only shows up in the

ground state energies of the clusters is equivalent to the assumption that F_{SH} does not depend on temperature. As seen in figs. 1 and 3, this is a reasonable assumption for clusters with a mass below 100. Above mass 300 there is a significant reduction of F_{SH} within the considered temperature range. Therefore, if one derives "shell energies" from the modulation of the evaporation yields, they do not represent the shell structure in the ground state separation energies. Rather, they should be understood as the differences $\Delta_1 F_{SH}$. In the case when T does not depend on N this is immediately clear from the rate expression (26) for large clusters.

As discussed by S. Bjørnholm in his lecture [20], the relationship between the intensities observed after the evaporation cascade and the rate constants is a complex one and the assumption that the temperature does not change with N is not correct. Nevertheless, it seems plausible that the "experimental shell energies" should be understood as *free* energies.

It would be interesting to use the rate constants derived on the basis of the SCM method for an analysis of the evaporation cascade. Since this remains to be carried out, we must restrict ourself to a qualitative discussion. Figs. 7 and 8 compare $\Delta_1 F_{SH}(T = 0.06eV, N)$ with $\ln(I_{rel})$, where I_{rel} are the experimental intensities [21] relative to a smooth background (for definition cf. S. Bjørnholms talk [20]). The shapes of the curves are remarkably similar. The magic number correspond to the intersections of the downsloping parts of $\Delta_1 F_{SH}$ with the zero line. These zeros agree well with the zeros of $\ln(I_{rel})$. The function $\Delta_1 F_{SH}$ has a horizontal section in the middle of each shell, which is a consequence of the deformation. The calculations for $T = 0.12\ eV$ in fig. 9 demonstrate that the horizontal section disappears for $N > 190$, where the calculated shapes are spherical. Flat sections in the middle of the shells are clearly visible in the experimental curves $\ln(I_{rel})$. They present evidence for the existence of deformation, in particular near mass 500 (cf. the discussion of the plasmon resonance in section 3).

In the experimental curves the shell structure is more washed out than in the calculations. It is also seen that the shell structure falls off faster with N in experiment than in theory. This has been discussed before in refs. [22, 9]. There is also the question of the absolute scale. Assuming that the intensities are proportional to the rate constant would ensue a scaling the experiment values $\ln(I_{rel})$ by T. With this scale the calculated shell modulation is a factor of 10 to 20 too large. As discussed by S. Bjørnholm [20], the analysis of the evaporation spectra by means of the model suggested by Hansen [23] seems the be a remedy to some of these problems. On the other hand, the shape of the curve $\ln(I_{rel})$ seems to correlate much better with the calculated curve $\Delta_1 F_{SH}$ than the experimental

curve $D(N)$ extracted from the intensities by means of this model.

5. Summary

We have generalized the shell correction approach to finite temperatures. A new renormalization procedure based on the canonical ensemble has been suggested. Renormalizing the smooth part of the free energy of the cluster to the free energy of a macroscopic droplet of liquid alkali metal implicitly includes the ionic degrees of freedom. This allows us to derive the density of states and a new expression for the evaporation rate of atoms, which we believe to be more accurate than the ones presently used. The free energy of sodium clusters in the mass range from 100 to 700 has been minimized with respect to several deformation parameters describing the axial shape of the cluster. For the clusters lying in the center of the open shells the deformation survives thermal fluctuations corresponding to temperatures of hot clusters forming the beam. The higher multipoles of the shape remain as important as for zero temperature but the regions of spherical shape around the magic numbers expand with increasing temperature and mass number.

The authors would like to thank S. Bjørnholm for stimulating discussions. Support by INTAS under the contract INTAS-93-151 is greatfully acknowledged.

References

[1] de Heer, W.A. (1993) *Rev. Mod. Phys.* **65**, 611.

[2] Strutinsky, V.M. (1967) *Nucl. Phys.* **A95**, 420; (1968) *Nucl. Phys.* **A122**, 1.

[3] Frauendorf, S. and Pashkevich, V.V. (in press) Proc. of ISSPIC7, Kobe 1994, *Surface Science Reviews and Letters*, preprint FZR-69.

[4] Landolt-Börnstein (1976) *Zahlenwerte und Funktionen aus Physik, Chemie, Astronomie, Geophysik und Technik*, Springer-Verlag, IV/2, p. 250.

[5] Knacke, O., Kubaschewski, O., and Hesselmann, K. (1991) *Thermochemical Properties of Inorganic Substances*, Springer, p. 1314.

[6] Frauendorf, S. and Pashkevich, V.V. (1993) *Z. Phys.* **D26**, S 98; *Phys. Rev.* **B**, submitted.

[7] Essebag, C. and Egido, J.L. (1993) *Nucl. Phys.* **A 552**, 205.

[8] Rossignioli R. *et al.* (1992) *Phys. Lett.* **B297**, 9.

[9] Brack, M. and Genzken, O. (1991) *Z. Phys.* **D21**, 65.

[10] Bréchignac, C., Cahuzac, Ph., Kebaïli, N., Leygnier, J., and Sarfati, A. (1992) *Phys. Rev. Lett.*, **26**, 3917.

[11] Weisskopf, V. (1937) *Phys. Rev.* **52**, 295.

[12] Engelking, P.C. (1987) *J. Chem. Phys.* **87**, 936.

[13] Klots, C. (1991) *Z. Phys.* **D 20**, 105.

[14] Hoare, M.R. and Ruijgrok, Th.W. (1970) J. Chem. Phys. **52**, 113.

[15] Frauendorf, S., *Z. Phys.* **D**, submitted.

[16] Hervieux, P.A. and Gross, D.H.E., *Z. Phys.* **D**, submitted.

[17] Hansen, K. and Manninen, M. (1994) *J. Chem. Phys.* **101**, 10481.

[18] Bréchignac, C., Cahuzac, Ph., Leygnier, J., and Weiner, J. (1989) *J. Chem. Phys.* **90**, 1492.

[19] Bréchignac, C., Busch, H., Cahuzac, Ph., and Leygnier, J. (1994) *J. Chem. Phys.* **101**, 6992.

[20] Bjørnholm, S., lecture at this conference.

[21] Torkildsen, F. *et al.*, to be published.

[22] Pedersen, J., Bjørnholm, S., Borggreen, J., Hansen, K., Martin, T.P., and Rasmussen, H.D. (1991) *Nature* **353**, 733.

[23] Hansen, K. (in press) Proc. of ISSPIC7, Kobe (1994), *Surface Science Reviews and Letters*.

Received by Publishing Department
on July 18, 1995.